Crack Front Waves and the Dynamics of a Rapidly Moving Crack

E. Sharon,[1] G. Cohen,[2] and J. Fineberg[2]
[1]*The Center for Nonlinear Dynamics, The University of Texas, Austin, Texas 78712*
[2]*The Racah Institute of Physics, The Hebrew University of Jerusalem, Jerusalem 91904, Israel*
(Received 19 July 2001; published 6 February 2002)

Crack front waves are nonlinear localized waves that propagate along the leading edge of a crack. They are generated by both the interaction of a crack with a localized material inhomogeneity and the intrinsic formation of microbranches. Front waves are shown to transport energy, generate surface structure, and lead to localized velocity fluctuations. Their existence locally imparts inertia, which is not incorporated in current theories of fracture, to initially "massless" cracks. This, coupled to microbranch formation, yields both inhomogeneity and scaling behavior within the fracture surface structure.

DOI: 10.1103/PhysRevLett.88.085503 PACS numbers: 62.20.Mk, 46.50.+a, 68.35.Ct

Dynamic fracture is of fundamental and practical importance. We consider the behavior of a crack interacting with a localized defect. We show that this interaction can induce fundamental changes to a crack's long-term dynamics. These changes imply that a necessarily 3D view of fracture must replace the basically 2D theory that is currently used to describe fracture in ideal materials.

In ideal (defect-free), brittle amorphous materials, experiments [1–3] indicate that until a crack bifurcates, its dynamic behavior is in excellent agreement with an equation of motion [4,5] based on a linear elastic description of a moving crack in a 2D material. Balancing the energy flux, G, per unit length of the crack with the fracture energy, Γ, defined as the energy needed to create a length of new fracture surface yields

$$G(v,l) \sim G(l)(1 - v/v_R) = \Gamma\,, \tag{1}$$

where v and v_R are, respectively, the instantaneous crack velocity and the Rayleigh wave speed of the material. $G(l)$ is dependent solely on the instantaneous crack length, l, and the loading conditions. As Eq. (1) has no inertial terms, a crack tip in a 2D material should behave as a massless, pointlike object. In ideal materials, Eq. (1) was shown [2] to break down when, beyond a critical velocity, v_c, a single crack loses stability [6–8] to a state in which a crack undergoes repetitive, short-lived microscopic branching ("microbranching") events (see, e.g., [9]).

Let us now consider the dynamics of a crack in a "nonideal" material populated by asperities (i.e., defects which locally perturb Γ). When a crack encounters an asperity, the system's translational invariance normal to the propagation direction (z axis in Fig. 1a) is broken. Thus, a crack tip can no longer be idealized as a pointlike object propagating within an, effectively, 2D material. The dynamics of the 1D front defined by the leading edge of the crack in a 3D material must now be considered. In this Letter we demonstrate that localized waves, "front waves," generated by an asperity, fundamentally affect a crack's dynamics. Front waves (FW) are elastic waves that propagate along a moving crack front. We show that these waves both transport energy along the crack front and locally impart inertia to the initially "massless" crack. This leads to a sharp localization of the energy flux at points along the front, as well as both self-perpetuating inhomogeneities and scaling of the fracture surface structure.

FW were first predicted as propagating velocity fluctuations confined to the fracture plane ($y = 0$ plane in Fig. 1a). Ramanathan and Fisher [10], building on work by Willis and Movchan [11,12], discovered that this new type of elastic wave is supported by the linearized equations describing the perturbed stress field of a moving crack. They are generated by asperities and propagate at velocities $0.94v_R < c_f < v_R$ relative to the asperity that produced them [10,13]. Thus, the FW velocity, $c_{||}$, along the propagating front is $c_{||} = \sqrt{c_f^2 - v^2}$. FW are stable for $\Gamma(v) = \text{const}$ and decay if $\Gamma(v)$ increases with v. FW were also observed numerically by Morrissey and Rice [13,14] and, under repeated interactions with asperities, were shown to lead to progressive roughening of the crack front profile, in agreement with previous predictions [15] of scalar models of fracture. Resonant effects of FW were anticipated in [16].

Recent experiments [17] in glass [where $\Gamma(v) \sim \text{const}$ [2]] have revealed that localized waves, whose propagation velocity corresponds to the predicted FW, are indeed emitted when a crack interacts with an asperity. The observed

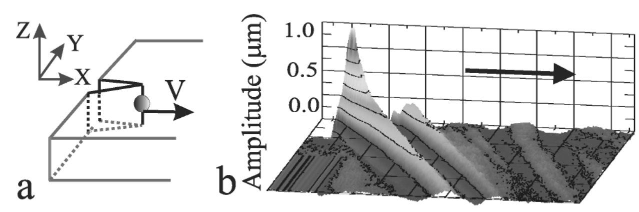

FIG. 1. (a) The translational symmetry along a crack front (z direction) is broken when the front (propagating in the x direction) encounters a localized asperity. (b) The interaction with a single asperity (located at the origin) produces a train of localized front waves that propagate along the front while generating tracks on the fracture surface. Shown is a fracture surface scan of a 1.5 mm × 1.5 mm section of the xz plane. The arrow indicates the front's direction of propagation.

 © 2002 The American Physical Society

waves have a distinct out-of-plane (y) component which leaves traces along the fracture surface (Fig. 1b). In addition, after an initial decay, FW rapidly converge to nondecaying long-lived waves with a unique characteristic profile. The FW scale is slightly less than the asperity size [17]. Their *shape,* however, is independent of initial conditions. FW retain this shape upon collisions, sustaining, as do solitons, a relative phase shift.

Our experiments were conducted in soda-lime glass plates of size $38 \times 44 \times 0.3$ cm in the x (propagation), y (loading), and z (sample thickness) directions, respectively (see Fig. 1a). As in [18], samples were loaded using quasistatic, mode I loading. Crack velocities at the plate surfaces (the $z = 0$ and $z = 0.3\ \mathrm{cm} \equiv z_{\max}$ planes) were measured with a resolution of 50 m/s. Surface amplitudes were measured using a modified Taylor-Hobson (Surtonic 3+) scanning profilometer with a 0.01 μm resolution normal to the fracture surface. Asperities were externally introduced within either the $z = 0$ or $z_{\max}$ planes by means of scribed lines of triangular cross section. These lines, whose scales ranged between 100–1000 μm, locally decreased Γ. Γ was locally increased when these lines were filled with superglue adhesive. FW were generated by both asperity types, and above $v_c = 0.42 v_R$ ($v_R = 3370$ m/s) by microbranching events.

As Fig. 1 indicates, the observed FW have a significant out-of-plane component. We now show that FW have an in-plane component: the velocity fluctuations predicted in [10,13,14]. Figure 2 shows the local velocity of the crack front on the plate face at $z = z_{\max}$ at locations where FW, launched from an asperity on the opposite face (the $z = 0$ plane), reached $z = z_{\max}$. The fracture surface amplitude is compared to the velocity fluctuations on this plane in Fig. 2a. In Fig. 2b this comparison is performed for FW generated by microbranching events. In both cases, velocity fluctuations of 20%–30% of the mean velocity correspond precisely to the arrival of the FW, as indicated by the surface height measurements.

We can estimate the normal velocity component $v_y \sim \delta y/\delta t$, using the surface amplitude, δy (where $\delta t \equiv \delta x/v$ for a pulse of spatial extent δx). v_y is less than 1% of the velocity fluctuations, v_x, in the propagation direction. Thus, the relatively small out-of-plane surface (velocity) variations generated by FW (which are undetectable in the velocity measurements) correspond to large local *in-plane* fluctuations of v.

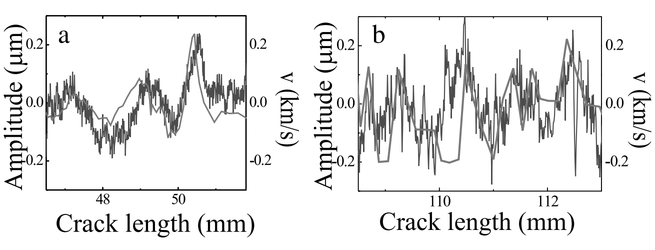

FIG. 2. Comparison, on the $z = z_{\max}$ plane, of velocity fluctuations (bold line) and the fracture surface height (thin line) generated by FW for (a) FW generated by an external asperity at $v = 1000$ m/s ($0.72 v_c$) and (b) FW generated by microbranching events at $v = 1500$ m/s ($1.08 v_c$). The velocity measurement resolution ($0.1\ \mu\mathrm{sec} \sim 0.05$–$0.1$ mm) was not sufficient to capture the fine structure of the surface measurements.

Assuming, as in [10,13,14], that Eq. (1) remains approximately valid, these data further indicate that FW transport significant amounts of energy along the front. Viewing Eq. (1) as valid locally along the front, local changes in v directly correspond to local changes in G. Thus the fluctuations in v, carried by FW along the front, transport the energy fluctuations generated locally by inhomogeneities. This transport of energy, due to FW, explains how experiments are *able* to measure velocity fluctuations when, generally, the measurement plane at $z = 0$ or $z_{\max}$ is situated relatively far from the microbranch events, located within the plate's interior, that initiated the fluctuations. Thus, the intrinsic velocity fluctuations measured in experiments are, in essence, front waves.

The strong correlation in both the amplitude and phase of the in-plane velocity measurements and the out-of-plane surface amplitudes indicates that these quantities can be regarded as two components of the same wave, rather than as two independent entities. These correlations suggest that significant coupling exists between in-plane and out-of-plane stress components at the crack front. As no *linear* coupling between in-plane and out-of-plane stress field components exists [12], the 3D nature of the FW is an indication of their nonlinear character. A further indication of FW nonlinearity is their characteristic shape. This shape is obtained for sufficiently large perturbations [17], whereas weak perturbations generate dispersive waves that rapidly decay.

In Fig. 3 we present the surface structure generated in the vicinity of a single asperity that was induced at $z = 0$. An initial FW is generated by the interaction of the crack front with an asperity and propagates away from its immediate vicinity. Additional FW are generated along the $z = 0$ plane *at times after* the interaction of the crack front with the asperity. As the initial FW, these then propagate away from their initiation points (generating the parallel tracks observed in Fig. 3a).

Defining W as the asperity's initial width, these additional FW originate at $2.3W$ intervals along the $z = 0$ plane (the FW origins were determined by the locations of the peak FW amplitudes along the $z = 0$ plane). Their initial amplitudes (Fig. 3b) exponentially decay with a decay length of $1.8W$. Thus, these additional FW indicate that the crack front ahead of the asperity retains a "memory" of its existence long after the initial FW has propagated away from the asperity. This suggests that, locally, the crack front experiences inertial effects.

The existence of these inertial effects is surprising in light of the predictions of 2D fracture mechanics. As Eq. (1) indicates, a local change in the fracture energy

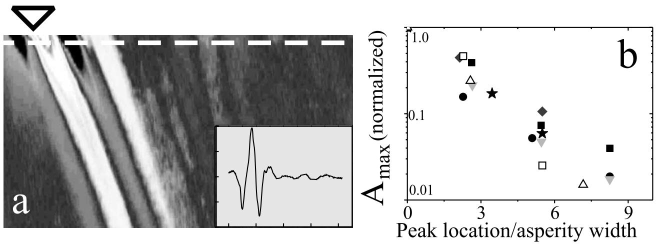

FIG. 3. (a) A train of propagating FW generated by a single asperity (its size and location indicated by the triangle). Shown are the data presented in Fig. 1b, projected onto the xz plane. White (black) corresponds to 1 μm (-1 μm). The crack front propagates from left to right. Dashed line: 1.6 mm long profile highlighted in the inset. Surface profile in the xy plane, showing the decay of the initial FW amplitudes. (b) The initial amplitude of each FW in the train exponentially decays with a characteristic decay length of $1.8W$, where W is the asperity width. Shown are the peak FW amplitudes $A_{\max}$ vs their distance from the asperity, normalized by W. Values of $W = 520$ μm (■), 500 μm (◆), 430 μm (▼), 410 μm (●), 170 μm (★), 160 μm (□), and 130 μm (△) were used.

should cause an immediate corresponding change in the instantaneous velocity of a crack. Therefore, the moment that a crack's tip passes an asperity's immediate vicinity, both G and v should instantly revert to their initial values, and no "memory effects" should be evident.

What is the origin of the periodicity of the FW train? This nontrivial behavior of the crack front ahead of the asperity suggests that by breaking the system's translational invariance along the crack front (z direction), the initially massless crack acquires inertia. A protrusion (indentation) can influence (be influenced by) other parts of the front via stress waves. As shown in [19] (for a static crack front), the local deviation, $\delta K(z)$, of the stress field intensity from that of a straight front is proportional to

$$\delta K(z) \propto \int_{-\infty}^{+\infty} [a(z') - a(z)]/(z' - z)^2 \, dz', \qquad (2)$$

where $a(z') - a(z)$ is the front's deviation in the x direction at point z along the front. The local value of $K(z)$ (the "stress intensity factor") is proportional to $G(z)^{1/2}$ and thereby [by Eq. (1)] drives the local front velocity. Thus, any part of the front that lags (overtakes) another will experience an increased (decreased) local stress that tends to stabilize a straight front. In the dynamic case, delayed potentials will introduce inertial effects [$a(z) \Rightarrow a(z,t)$ and $K(z) \Rightarrow K(z,t)$] thereby giving rise to oscillatory behavior of the local stress field [14]. Numerical evidence for a local increase of the stress field was provided in [13], where a local increase of the front velocity was observed directly ahead of an asperity. The characteristic time scale for stress oscillations is [14] the time, $W/c_{\|}$, in which a front wave, traveling along the front with velocity $c_{\|} = \sqrt{c_f^2 - v^2}$, traverses an asperity of size W. Thus, the front immediately ahead of the asperity feels the effects of the oscillating stress field at a spatial scale of $Wv/c_{\|} = Wv/\sqrt{c_f^2 - v^2}$. This scale is consistent with the observed scaling of both the decay length (Fig. 3b) and spatial periodicity (Figs. 3a and 4c) of the structure formed ahead of an asperity.

Below the microbranching instability ($v < v_c$) the surface structure described in Fig. 3 is typical of that generated by the interaction of a crack front with an asperity. Above v_c, as shown in Fig. 4, microbranching events [17] themselves serve as FW sources since, like an asperity, they effectively increase the local value of the fracture energy. Microbranches, once excited, are the source of significant surface structure. Microbranches in glass are *not* randomly dispersed throughout the fracture surface but, as shown in Fig. 4a, are aligned along straight lines, "branch lines," in the propagation direction. Their internal structure (Figs. 4b and 4c) indicates rough periodicity in x [20]. As a consequence of the increased surface area created by the microbranches [18] upon branch-line formation, the energy flux, G, into the front is not evenly distributed along the front. The total energy dissipated by a branch line at a given location, z, along the front can be significantly larger than in the surrounding, featureless surface. This inhomogeneous distribution of G, which is perpetuated for the life of a branch line, indicates a nonlinear focusing of energy in the z direction that is not inherent in current theories of fracture. As shown in Fig. 4a, multiple branch lines can coexist, although they have a tendency to coalesce. These lines [18,20,21] are either initiated spontaneously or can be triggered by an asperity. We now show that the branch lines and their

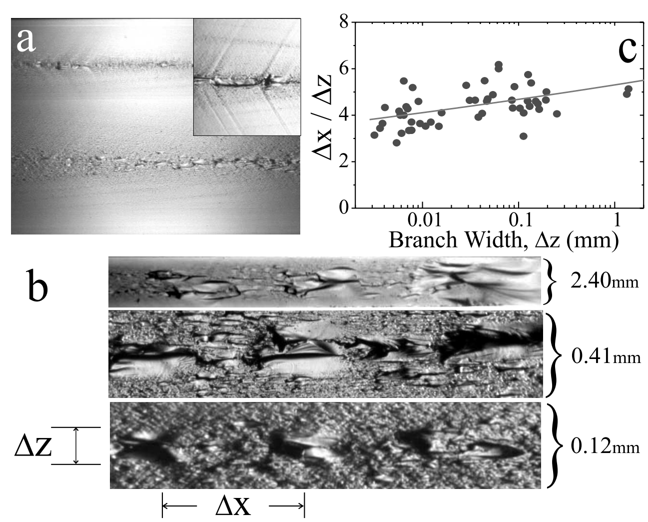

FIG. 4. (a) Photograph (of width 4 mm) of two parallel branch lines. (Inset) FW emitted from a branch line. Branch lines are formed (b) by periodic arrays of microbranches at many scales. Respective photograph scales (in mm) are noted. (c) The period, Δx, roughly scales with the branch-line width, Δz. The predicted dependence of $\Delta z/\Delta x$ (line), where the scale in x is determined by the propagation time of a FW across the branch-line width. Crack propagation in (a) and (b) was from left to right.

scaling properties directly result from the inertia acquired by the crack.

Let us consider the behavior of a crack front immediately after a perturbation of width W (either a microbranch event or an asperity) is encountered. At the conclusion of this event the local velocity of the crack front, ahead of the perturbation, will momentarily "overshoot" its unperturbed velocity v (see [13] and Fig. 3). For $v < v_c$, the overshoot will exponentially "ring down" as in Fig. 3. For $v > v_c$ the velocity overshoot will not decay. Since v is locally above the branching instability threshold, it will instead initiate another branching event, directly ahead of the first microbranch/asperity. This scenario will again repeat itself, thereby generating yet another branching event. In this picture, columns of branches spaced $Wv/\sqrt{c_f^2 - v^2}$ apart, in the propagation direction, will be generated. This scaling behavior is shown in Fig. 4b. The initial scale, W, of the branch lines is dynamically determined by G, as demonstrated in [18,22], where W is a roughly exponential function of v. As Fig. 4c indicates, this scaling behavior is indeed observed for over 3 orders of magnitude in W. The systematic increase with v of microbranch periodicity, apparent in the figure, is consistent with the predicted $v/\sqrt{c_f^2 - v^2}$ behavior. Note that when $v \sim v_c$ the above picture predicts that an asperity should initiate a branch line. Slowly decaying branch lines initiated by an asperity are indeed observed in [21] near v_c. Thus, branch-line formation and the overshoots described in Fig. 3 are different manifestations of the inertial effects associated with FW formation. On the other hand, when FW decay rapidly (e.g., polymethylmethacrylate), branch lines are *not* observed and the surface structure formed by microbranches is randomly distributed along the fracture surface.

In conclusion, we have demonstrated that FW both transport energy along a crack front and consist of coupled in-plane and out-of-plane components. The broken translational symmetry along the front gives rise to local inertia of the front. This local inertia, when coupled to the microbranching instability, provides a mechanism for the generation of stable, directed lines of spatially periodic microbranches in the propagation direction. This picture, which yields an explanation of both branch-line periodicity and scaling, may provide insight on the dynamic origins of fracture surface roughness [23]. Both the effective focusing, by branch lines, of energy within the crack front and the spontaneous birth of local inertia within a crack front point to fundamental features of crack dynamics that can not be incorporated into the current 2D descriptions of fracture. These may point to the need for a fundamentally new theory of fracture.

J. F. and G. C. acknowledge the support of the MAFAT development fund.

[1] H. Bergkvist, Eng. Fract. Mech. **6**, 621 (1974).
[2] E. Sharon and J. Fineberg, Nature (London) **397**, 333 (1999).
[3] B. Q. Vu and V. K. Kinra, Eng. Fract. Mech. **15**, 107 (1981).
[4] L. B. Freund, *Dynamic Fracture Mechanics* (Cambridge University Press, Cambridge, 1990).
[5] J. D. Eshelby, Sci. Prog. (Northwood, UK) **59**, 161 (1971).
[6] J. Fineberg, S. Gross, M. Marder, and H. Swinney, Phys. Rev. Lett. **67**, 457 (1991).
[7] J. F. Boudet, S. Ciliberto, and V. Steinberg, J. Phys. II (France) **6**, 1493 (1996).
[8] T. Cramer, A. Wanner, and P. Gumbsch, Phys. Rev. Lett. **85**, 788 (2000).
[9] J. Fineberg and M. Marder, Phys. Rep. **313**, 1 (1999).
[10] S. Ramanathan and D. S. Fisher, Phys. Rev. Lett. **79**, 877 (1997).
[11] J. R. Willis and A. B. Movchan, J. Mech. Phys. Solids **43**, 319 (1995).
[12] J. R. Willis and A. B. Movchan, J. Mech. Phys. Solids **45**, 591 (1997); A. B. Movchan, H. Gao, and J. R. Willis, Int. J. Solids Struct. **35**, 3419 (1998).
[13] J. W. Morrissey and J. R. Rice, J. Mech. Phys. Solids **46**, 467 (1998).
[14] J. W. Morrissey and J. R. Rice, J. Mech. Phys. Solids **48**, 1229 (2000).
[15] G. Perrin and J. R. Rice, J. Mech. Phys. Solids **42**, 1047 (1994); J. R. Rice, Y. Ben-Zion, and K. S. Kim, J. Mech. Phys. Solids **42**, 813 (1994); Y. Ben-Zion and J. W. Morrissey, J. Mech. Phys. Solids **43**, 1363 (1995).
[16] J. F. Boudet and S. Ciliberto, Physica (Amsterdam) **142D**, 317 (2000).
[17] E. Sharon, G. Cohen, and J. Fineberg, Nature (London) **410**, 68 (2001).
[18] E. Sharon and J. Fineberg, Phys. Rev. B **54**, 7128 (1996).
[19] J. R. Rice, J. Appl. Mech. **52**, 571 (1985).
[20] E. K. Beauchamp, J. Am. Ceram. Soc. **78**, 689 (1995).
[21] A. Tsirk, in *Advances in Ceramics: Fractography of Glasses and Ceramics,* edited by J. Varner and V. Frechette (The American Ceramic Society, Westerville, OH, 1988), Vol. 22, pp. 57–69.
[22] E. Sharon and J. Fineberg, Philos. Mag. B **78**, 243 (1998).
[23] E. Bouchaud, G. Lapasset, J. Planes, and S. Naveos, Phys. Rev. B **48**, 2917 (1993); K. J. Maloy, A. Hansen, E. L. Hinrichsen, and S. Roux, Phys. Rev. Lett. **68**, 213 (1992).